Postprint of: Kumar Jena S., Chakraverty S., Malikan M., Sedighi H. M.: Hygro-Magnetic Vibration of the Single-Walled Carbon Nanotube with Nonlinear Temperature Distribution Based on a Modified Beam Theory and Nonlocal Strain Gradient Model. INTERNATIONAL JOURNAL OF APPLIED MECHANICS Vol. 12 No. 5 (2020), 2050054 (29 pages).
DOI: 10.1142/S1758825120500544

JOURNAL URL: https://www.worldscientific.com/

HYGRO-MAGNETIC VIBRATION OF THE SINGLE-WALLED CARBON NANOTUBE WITH NONLINEAR TEMPERATURE DISTRIBUTION BASED ON A MODIFIED BEAM THEORY AND NONLOCAL STRAIN GRADIENT MODEL

Subrat Kumar Jena[1], S. Chakraverty[2]*, Mohammad Malikan[3], Hamid Mohammad-Sedighi[4,5]

[1, 2]*Department of Mathematics, National Institute of Technology Rourkela, 769008, India*

[3]*Department of Mechanics of Materials and Structures, Faculty of Civil and Environmental Engineering, Gdansk University of Technology, P.O. Box 80-233 Gdansk, Poland*

[4]*Mechanical Engineering Department, Faculty of Engineering, Shahid Chamran University of Ahvaz, Ahvaz, P.O. Box 61357-43337, Iran*

[5]*Drilling Center of Excellence and Research Center, Shahid Chamran University of Ahvaz, Ahvaz, Iran*

**Corresponding author*

E-mail: *[1]sjena430@gmail.com, [2]sne_chak@yahoo.com, [3]mohammad.malikan@pg.edu.pl, [4]h.msedighi@scu.ac.ir*

Abstract

In this study, vibration analysis of single-walled carbon nanotube (SWCNT) has been carried out by using a refined beam theory, namely one variable shear deformation beam theory. This approach has one variable lesser than a contractual shear deformation theory such as first-order shear deformation theory (FSDT) and acts like classical beam approach but with considering shear deformations. The SWCNT has been placed in an axial or longitudinal magnetic field which is also exposed to both the hygroscopic as well as thermal environments. The thermal environment is considered as nonlinear thermal stress field based on the Murnaghan's model whereas the hygroscopic environment is assumed as a linear stress field. The size effect of the SWCNT has been captured by both the nonlocal and gradient parameters by employing the Nonlocal Strain Gradient Theory (NSGT). Governing equation of motion of the proposed model has been developed by utilizing the extended Hamilton's principle and the non- dimensional frequency parameters have been computed by incorporating the Navier's approach for Hinged-Hinged (HH) boundary condition. The proposed model is validated with the existing model in special cases, by comparing the non- dimensional frequency parameters, displaying an excellent agreement. Further, a parametric study has been conducted to analyze the impact of nonlocal parameter, gradient parameter, thermal environment, hygroscopic environment, and magnetic field intensity on the non-dimensional frequency parameters. Also, results for some other theories like Classical Elasticity Theory (CET), Nonlocal Elasticity Theory (NET), and Strain Gradient Theory (SGT) have been presented along with the NSGT.

Keywords: SWCNT; Hygroscopic environment; Nonlinear thermal stress; Magnetic field; NSGT; New refined beam theory.

1. Introduction

Humidity sensors are now widely used in industrial processes and environmental control. For manufacturing high precision circuits in the semiconductor industry, the level of humidity in the manufacturing process is monitored. Figure 1 shows the schematic representation of a CNT-based humidity sensor fabricated from suspended nanotube. Fig. 2a also illustrates the schematic diagram of another humidity sensor composed of anode CNT on a silicon plate and cathode ITO film glass plate which are insulated by a glass frame. As shown in Fig. 2b, the measurement method of the mentioned nanotube-based sensor installed above a cup of saturated fluid in which biased DC voltage can be applied between the cathode and anode and the air in the container is pumped out.

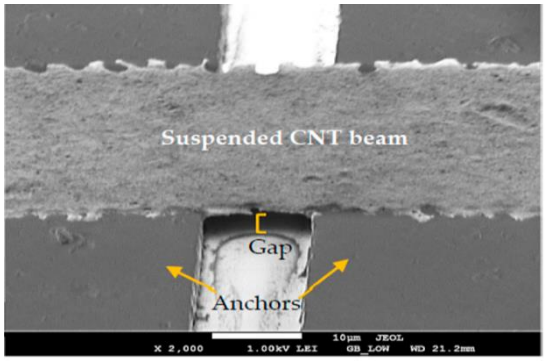

Fig. 1. SEM image of the suspended humidity sensor CNT [Arunachalam *et al.*, 2019]

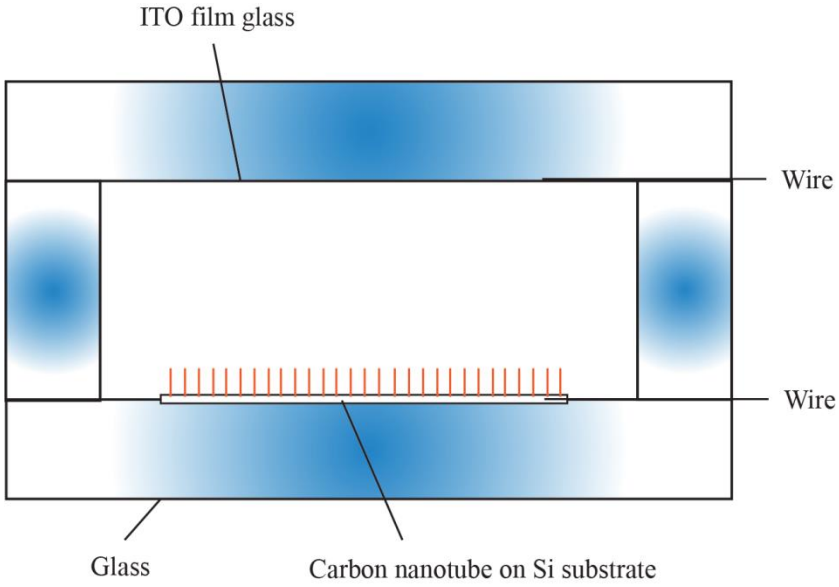

Fig. 2a. Schematic configurations of the sensor device [Huang *et al.*, 2009]

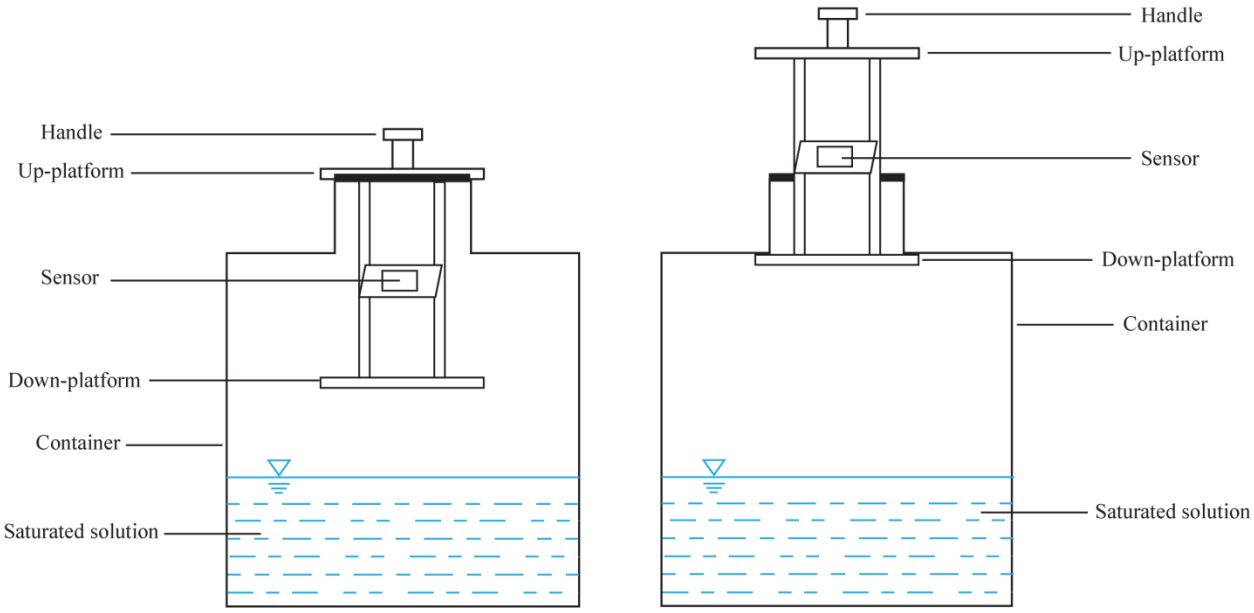

Fig. 2b. Schematic configurations of the measurement method [Huang *et al.*, 2009]

There are also many home applications such as intelligent control of the environmental features of buildings, baking control for microwave ovens, intelligent control of the washing machine, as well as in the automotive industry humidity sensors are used in the glass detergent system and motor assembly lines. In the medical field, humidity sensors are used in respiratory equipment, sterilizers, early childhood growth chambers, medicine manufacturing processes, and biological products. In agriculture, moisture sensors are used to ventilate greenhouses, protect plants (prevent dew), measure soil moisture, and store cereals. In the industry in general, humidity sensors are used to control humidity in the purification of chemical gases, dryers, ovens, thin films, and feed processes. Humidity sensors must have conditions such as high sensitivity to humidity and short response time, high service life, durability, and mechanical strength, appropriate temperature dependence, and resistance to contamination [Cao *et al.*, 2011; Moraes *et al.*, 2014; Ma *et al.*, 1995; Arunachalam *et al.*, 2018]. To date, various structures have been proposed for the construction of humidity sensors. But it can be truly stated that carbon nanotubes (CNTs) in single-walled (SWCNTs) and multi-walled (MWCNTs) structures can be one of the best types of structures used for moisture sensors [Zhao *et al.*, 2011; Han *et al.*, 2012; Jung *et al.*, 2014; Quelennec *et al.*, 2019].

To predict statically and dynamically the behavior of micro/nanoscale structures and devices, there have been demonstrated various ways, such as molecular mechanics [Ansari et al., 2012], equivalent energy method [Mohamed *et al*., 2020; Eltaher *et al*., 2019a], multi-scale homogenization [Ebrahimi and Dabbagh, 2019], and elasticity continuum mechanic. The continuum approaches are the costly and simpler available theories. Within these hypotheses, first and second strain gradients of Mindlin [Mindlin, 1965, Mindlin and Eshel, 1968; Akgöz and Civalek, 2014], and couple stress theories [Akgöz and Civalek, 2012; Zeighampour and Tadi Beni, 2014; Eltaher *et al*., 2018; Malikan, 2017] can show size-dependent response of micro/nanostructures. Though these theories are unable to give nonlocality for the atomic lattice. On the other side, nonlocality is another discovered phenomenon of nanoscale size which declares that stress into an atom is related to strain in all atoms in the atomistic domain. This hypothesis is a well-known approach named as nonlocal elasticity theory formulated by Eringen and has been being used exceedingly [Eringen, 1972; Aydogdu and Filiz, 2011; Demir and Civalek, 2014; Ansari and Gholami, 2014; Islam *et al*., 2014; Numano□lu *et al*., 2015; Jena *et al.*, 2020a, 2020b]. There is also a combination of these approaches called nonlocal strain gradient theory presented by Lim *et al*. [2015]. According the idea done by these researchers, a nanostructure apart from stress nonlocality, needs strain gradients. Because deformations of atoms also present gradients of strain as strain in the center of atoms will be different with the top or bottom and therefore there is a rate for variations of strain throughout the thickness. There is also another type of nonlocal continuum model known as stress-driven nonlocal elasticity [Apuzzo *et al*., 2018; Barretta *et al*., 2020; Luciano *et al*., 2020; Barretta, and Marotti de Sciarra, 2018]. Moreover, there are several other properties for nanomaterials that have been known so far, such as surface elasticity [Eltaher *et al*., 2019b].

In the case of humidity, thermal, and magnetic conditions analysis of CNTs and nanobeams, attempts to predict the durability, stability, and mechanics of CNTs have been spread over the current decade [Kraus, 1984; Zhen and Fang, 2010; Maachou *et al.*, 2011; Kiani, 2012; Narendar *et al.*, 2012; Pradhan and Mandal, 2013; Li *et al.*, 2016; Mohammadi *et al.*, 2016; Ma *et al.*, 2017; Ebrahimi and Barati, 2017a, 2017b; Chang, 2017; Jena and Chakraverty, 2018; Jena and Chakraverty, 2019; Kiani, 2018; Malikan *et al.*, 2018a; Alibeigi *et al.*, 2018; Malikan *et al.*, 2019; Zhen *et al.*, 2019; Karami *et al.*, 2019; Barati *et al.*, 2019; Jena *et al.*, 2019a, 2019b, 2019c]. However, there are already many gaps to fill the studies about the mechanical analysis of CNTs. In terms of the literature and close published works, Ponnusamy and Amuthalakshmi [2015] investigated the effects of magnetic and thermal environments on natural frequencies of a double-walled carbon nanotube (DWCNT) based on the Timoshenko beam hypothesis. The nonlocal approach of Eringen was considered for the model to examine nanoscale impacts. Zidour *et al.* [2012] studied the influence of temperature of the environment on the dynamic response of the Zigzag carbon nanotubes based on the Timoshenko beam approach in a nonlocal domain. Ebrahimi and Barati [2017a] performed hygro and thermal influences on the vibrational response of a nanobeam. The beam was assumed as temperature-dependent material, and the effect of material nonhomogeneity was also taken into consideration. They used three kinds of thermal distributions, namely linear, uniform and sinusoidal temperature changes. Besides, the Euler-Bernoulli kinematic beam approach was employed to present the equations of motion. Mouffoki *et al.* [2017] analyzed the vibration behavior of a nanobeam on the basis of the nonlocal continuum model subjected to humidity and temperature changes. They used a refined two-trigonometric shear deformation model in order to capture the formulation. Three kinds of distributions for the thermal environment were applied, namely, sinusoidal, uniform and linear thermal in-plane forces. The nanobeam was also assumed as a functional material. Jouneghani *et al.* [2018] modeled a nanobeam in a thermo-hygral environment with considering material porosity in order to calculate the static bending deflections. The nanoscale influence was taken on the basis of continuum nonlocal theory. Arefi and Soltan Arani [2018] investigated a fully environmental effect consisting of electric, magnetic, humidity, and temperature changes on the deflection analysis of a nanobeam which incorporated a functional property. The constitutive equations were derived on the basis of a higher-order beam model, namely the third-order shear deformation approach. Dini *et al.* [2019] developed the studies on the hygrothermal effects of CNTs by presenting research on the dynamics of DWCNTs under magnetic, thermal and humidity surroundings. They utilized the field of Euler-Bernoulli in order to extract the basic equations. The nonlocality was evaluated based on the model of Eringen. Jalaei *et al.* [2019] recently presented the influences of thermal and magnetic fields on the dynamic instability of a nonlocal strain gradient beam based on the Timoshenko beam hypothesis. Habibi *et al.* [2019] conducted research on a nanobeam located in a thermo-electro-magneto-elastic environment on the basis of the Euler-Bernoulli kinematic displacement field. They developed the model in a small-scale region regarding the modified couple stress theory. Ebrahimi-Nejad *et al.* [2019] studied the effects of thermo-mechano-hygral environments for considering small scale influences for vibrations analysis of a nanobeam, which included functional property. They implemented a porosity into the model and derived their mathematical relations based on the Eringen's stress nonlocality and classic beam approach. The numerical outcomes were also presented on the basis of different edge conditions. Arani *et al.* [2015] studied flexular vibration stability of double walled viscoelastic carbon nanotube carrying fluid by using Timoshenko beam model. The nanotube was embedded in Pasternak elastic foundation while Vander Waals (vdW) force of attraction between the inner and outer layer of the nanotube was taken into consideration as per Lenard-Jones model. In the work of Yazdani *et al.* [2019], vibration characteristics of Cooper-Naghdi micro sandwich cylindrical shell were studied considering saturated porous core with reinforced carbon nanotube piezoelectric composite face sheets with help of first order shear deformation theory and modified couple stress theoy.

To the best of authors knowledge, no research was found where mechanical behavior of carbon nanotubes are studied by considering thermal environment as nonlinear thermal stress field based on the Murnaghan model and hygroscopic environment based on a linear stress field. All the published lieratures close to the present work were reviewed, some of which may not be mentioned in this article due to the large volume of references. To this end, the authors are motivated to study free vibration of SWCNT placed in an axial magnetic field subjected to hygro-thermal environment assuming nonlinear thermal stress field based on the Murnaghan model. A modified beam model, namely, one variable shear deformation beam theory is used to investigate the displacement field of the beam. Size-dependant effect of the CNT has been captured by nonlocal strain gradient theory (NSGT) and other special cases such as Classical Elasticity Theory (CET), Nonlocal Elasticity Theory (NET), and Strain Gradient Theory (SGT) have also been encorporated. Further, a parametric analysis is carried out to investigate the influence of nonlocal parameter, gradient parameter, thermal environment, hygroscopic environment, and magnetic field

intensity on the non-dimensional frequency parameters by using graphical results employing Navier's technique for HH boundary condition.

2. Formulation of Proposed Model

In this investigation, a zigzag type of SWCNT of length L, thickness h, and diameter d has been exposed to hygro-thermal-magneto environments with nonlinear temperature distribution based on the Murnaghan model. The schematic diagram of this model is illustrated in Fig. 3. In the upcoming subsection, reviews of NSGT, Maxwell's relations, and hygro-thermal environments have been summarized and the proposed model is developed.

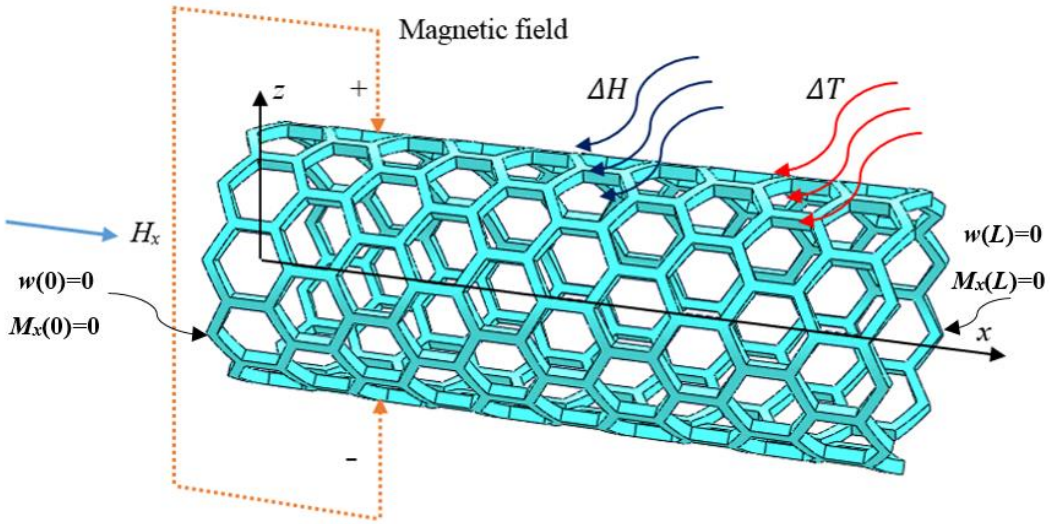

Fig. 3 Schematic diagram of zigzag type SWCNT subjected to hygro-thermal-magneto environments

2.1. Review of the nonlocal strain gradient theory

Total stress field tensor, as per the nonlocal strain gradient theory [Lim *et al.*, 2015; Li *et al.*, 2016; Lu *et al.*, 2017; Khaniki and Hosseini-Hashemi, 2017; Jena *et al.*, 2019d], depends on not only classical nonlocal stress tensor but also on higher-order nonlocal stress tensor which is presented as

$$t = \sigma - \nabla\sigma^{\bullet}, \tag{1}$$

where $\sigma = \int_0^L E\alpha(x,x',e_0a)\varepsilon'_{xx}(x')dx'$ and $\sigma^{\bullet} = l^2\int_0^L E\alpha^*(x,x',e_1a)\varepsilon'_{xx,x}(x')dx'$ are the classical nonlocal stress tensor and the higher-order nonlocal stress tensor, respectively. $\alpha(x,x',e_0a)$ and $\alpha^*(x,x',e_1a)$ represent the nonlocal kernels, ε_{xx} and $\varepsilon_{xx,x}$ represent the strain tensor and gradient of the strain tensor, L and l denote the external characteristics length of the beam and gradient parameter, and e_0a, and e_1a are the nonlocal parameters due to the higher-order strain gradient stress field. Applying the nonlocal differential operator $\left(\ell_i = 1-(e_ia)^2\nabla^2, i=0,1\right)$ on the stress field defined in Eq.(1), we obtain [Lim *et al.*, 2015; Li *et al.*, 2016; Lu *et al.*, 2017; Khaniki and Hosseini-Hashemi, 2017; Jena *et al.*, 2019d; Malikan, 2020; Malikan *et al.*, 2020]

$$\left(1-(e_0a)^2\nabla^2\right)\left(1-(e_1a)^2\nabla^2\right)t_{xx} = E\left(1-(e_1a)^2\nabla^2\right)\varepsilon_{xx} - El^2\left(1-(e_0a)^2\nabla^2\right)\nabla^2\varepsilon_{xx} \tag{2}$$

Assuming $e_0a = e_1a$, the first order nonlocal strain gradient model for 1D elastic material will be modified as

$$\left(1-(e_0a)^2\frac{\partial^2}{\partial x^2}\right)t_{xx}=E\left(1-l^2\frac{\partial^2}{\partial x^2}\right)\varepsilon_{xx} \tag{3a}$$

$$\left(1-(e_0a)^2\frac{\partial^2}{\partial x^2}\right)t_{xz}=G\left(1-l^2\frac{\partial^2}{\partial x^2}\right)\gamma_{xz} \tag{3b}$$

2.2. Review of Maxwell's relations

From Maxwell's relations, we have [Kraus, 1984; Narendar *et al.*, 2019; Ebrahimi and Barati, 2017a]

$$\begin{aligned} &J=\nabla\times h,\ \nabla\times e=-\eta\frac{\partial h}{\partial t},\nabla h=0,\\ &e=-\eta\left(\frac{\partial U}{\partial t}\times H\right),h=\nabla\times(U\times H)\end{aligned} \tag{4}$$

Here J is the current density vector, h is the initially applied disturbance to the magnetic field, e denotes the strength of the electric field, η symbolizes the magnetic permeability, $H=(H_x,0,0)$ is the applied longitudinal magnetic field vector on SWCNT, and $U=(u,v,w)$ represents the displacement field vector of the SWCNT.

Using Eq. (4), we now obtain

$$h=\nabla\times(U\times H)=-H_x\left(\frac{\partial v}{\partial y}+\frac{\partial w}{\partial z}\right)\hat{i}+H_x\frac{\partial v}{\partial x}\hat{j}+H_x\frac{\partial w}{\partial x}\hat{k} \tag{5}$$

$$J=\nabla\times h=H_x\left(\frac{\partial^2 w}{\partial x\partial y}-\frac{\partial^2 v}{\partial x\partial z}\right)\hat{i}-H_x\left(\frac{\partial^2 v}{\partial y\partial z}+\frac{\partial^2 w}{\partial x^2}+\frac{\partial^2 w}{\partial z^2}\right)\hat{j}+H_x\left(\frac{\partial^2 w}{\partial y\partial z}+\frac{\partial^2 v}{\partial x^2}+\frac{\partial^2 v}{\partial y^2}\right)\hat{k} \tag{6}$$

The Lorentz force induced by applied longitudinal magnetic field vector may be written as [Kraus, 1984; Narendar *et al.*, 2019; Ebrahimi and Barati, 2017a]

$$f=\eta(J\times H)=\eta\left[H_x^2\left(\frac{\partial^2 v}{\partial x^2}+\frac{\partial^2 v}{\partial y^2}+\frac{\partial^2 w}{\partial y\partial z}\right)\hat{j}+H_x^2\left(\frac{\partial^2 w}{\partial x^2}+\frac{\partial^2 w}{\partial y^2}+\frac{\partial^2 v}{\partial y\partial z}\right)\hat{k}\right] \tag{7}$$

Now, the resultant Lorentz force in the z-direction can be obtained as [Kraus, 1984; Narendar *et al.*, 2019; Ebrahimi and Barati, 2017a]

$$f_{Lz}=\eta\int_A f_z dA=\eta A H_x^2\frac{\partial^2 w}{\partial x^2} \tag{8}$$

2.3. Review of Hygrothermal environment

Based on thermal elasticity theory, the axial force due to the thermal environment $\left(N^T\right)$ can be given as [Je¸kot, 1996; Mohammadi *et al.*, 2016; Takahashi, 2018]

$$N^T=-\int_A\Phi(\Delta T)dA \tag{9}$$

in which $\Phi(\Delta T)$is the nonlinear elastic stress temperature coefficient, which may be defined as [Je¸kot, 1996; Mohammadi *et al.*, 2016; Takahashi, 2018]

$$\Phi(\Delta T)=E\alpha_x\Delta T-\hat{h}\alpha_x^2\Delta T^2\quad\text{with}\quad\hat{h}=l_1(1-2\upsilon)-2m_1\left(\upsilon^2-1\right)+n_1\upsilon^2 \tag{10}$$

where ΔT is the change in temperature, α_x is the coefficient of thermal expansion, $(l_1,m_1,n_1)$are Murnaghan's third-order elastic constant, E is Young's modulus and υ is the Poisson's ratio.

Substituting Eq. (10) into Eq. (9), we obtain [Je¸kot, 1996; Mohammadi *et al.*, 2016; Takahashi, 2018]

$$N^T = -\int_A \Phi(\Delta T)dA = -\int_A \left(E\alpha_x \Delta T - \hat{h}\alpha_x^2 \Delta T^2\right)dA = -\left(EA\alpha_x \Delta T - A\hat{h}\alpha_x^2 \Delta T^2\right) \tag{11}$$

According to Hygroscopic elasticity theory, the axial force due to the Hygroscopic environment $\left(N^H\right)$ can be presented as [Je¸kot, 1996; Mohammadi *et al.*, 2016; Takahashi, 2018]

$$N^H = -\int_A \phi(\Delta H)dA \tag{12}$$

Here $\phi(\Delta H)$ is the elastic stress due to Hygroscopic environment, which is defined as [Je¸kot, 1996; Mohammadi *et al.*, 2016; Takahashi, 2018]

$$\phi(\Delta H) = E\beta_x \Delta H \tag{13}$$

in which β_x denotes the hygroscopic expansion coefficient, and ΔH is the change in moisture concentration.

Plugging Eq. (13) into Eq. (12), we have [Je¸kot, 1996; Mohammadi *et al.*, 2016; Takahashi, 2018]

$$N^H = -\int_A \phi(\Delta H)dA = -\int_A \left(E\beta_x \Delta H\right)dA = -EA\beta_x \Delta H \tag{14}$$

2.4. Governing equations of motion for the proposed model

According to the new refined beam theory [Malikan *et al.*, 2019], there is a possibility to derive a new beam theory in a combination of first-order shear deformation theory and simple beam/plate theory [Thai *et al*., 2016]. There can also be seen other efforts to gain a beam theory from another one by some researchers [Barretta, 2012, 2013, 2014; Romano *et al*., 2012]. They derived a view of first-order shear deformation theory based on the Saint-Venant beam model.

The displacement fields can be expressed as [Malikan *et al.*, 2019]

$$\begin{aligned} u_1(x,z,t) &= u(x,t) - z\frac{\partial w(x,t)}{\partial x} \\ u_2(x,z,t) &= 0 \\ u_3(x,z,t) &= w(x,t) + B\frac{\partial^2 w(x,t)}{\partial x^2} \end{aligned} \tag{15}$$

Here $u(x,t)$ and $w(x,t)$ are the displacements of the neutral axis in axial and transverse directions, respectively. $B = \frac{EI}{AG}$, where E is Young's modulus, $I = \int_A z^2\, dA$ is the moment of area, A is the area of cross-section, and G is the shear modulus.

The strain displacement relations due to the new refined beam theory are given as

$$\varepsilon_{xx} = \frac{\partial u}{\partial x} - z\frac{\partial^2 w}{\partial x^2},\ \gamma_{xz} = B\frac{\partial^3 w}{\partial x^3} \tag{16}$$

Considering the axial strain due to hygrothermal environments, Eq. (16) will be converted into

$$\begin{aligned} \varepsilon_{xx} &= \frac{\partial u}{\partial x} - z\frac{\partial^2 w}{\partial x^2} - \left(\alpha_x \Delta T - \frac{\hat{h}\alpha_x^2 \Delta T^2}{E}\right) - \beta_x \Delta H, \\ \gamma_{xz} &= B\frac{\partial^3 w}{\partial x^3} \end{aligned} \tag{17}$$

The virtual strain energy (δU) for SWCNTs may be written as

$$\begin{aligned}\delta U &= \iiint_V \left(\sigma_{xx}\delta\varepsilon_{xx} + \sigma_{xx}^{(1)}\nabla\delta\varepsilon_{xx} + \sigma_{xz}\delta\gamma_{xz} + \sigma_{xz}^{(1)}\nabla\delta\gamma_{xz}\right)dV \\ &= \iiint_V \left[\left(\sigma_{xx} - \nabla\sigma_{xx}^{(1)}\right)\delta\varepsilon_{xx} + \left(\sigma_{xz} - \nabla\sigma_{xz}^{(1)}\right)\delta\gamma_{xz}\right]dV \\ &= \int_0^L \left[N_{xx}\frac{\partial\delta u}{\partial x} - M_{xx}\frac{\partial^2\delta w}{\partial x^2} + Q_{xz}B\frac{\partial^3\delta w}{\partial x^3}\right]dx \\ &= \int_0^L \left[-\frac{\partial N_{xx}}{\partial x}\delta u - \frac{\partial^2 M_{xx}}{\partial x^2}\delta w - B\frac{\partial^3 Q_{xz}}{\partial x^3}\delta w\right]dx\end{aligned} \tag{18}$$

where $M_{xx} = \int_A z(\sigma_{xx})dA$, $N_{xx} = \int_A (\sigma_{xx})dA$, and $Q_{xz} = \int_A (\sigma_{xz})dA$ are the local stress resultants of the beam.

The virtual kinetic energy (δT) of the nanotube can be written as

$$\begin{aligned}\delta T &= \frac{1}{2}\rho\iiint_v \left[\delta\left\langle\left(\frac{\partial u_1}{\partial t}\right)^2 + \left(\frac{\partial u_2}{\partial t}\right)^2 + \left(\frac{\partial u_3}{\partial t}\right)^2\right\rangle\right]dV \\ &= \int_0^L \left[\begin{array}{l} I_0\frac{\partial u}{\partial t}\frac{\partial\delta u}{\partial t} + I_2\frac{\partial^2 w}{\partial x\partial t}\frac{\partial^2\delta w}{\partial x\partial t} + I_0\frac{\partial w}{\partial t}\frac{\partial\delta w}{\partial t} + \\ I_0 B\frac{\partial w}{\partial t}\frac{\partial^3\delta w}{\partial x^2\partial t} + I_0 B\frac{\partial^3 w}{\partial x^2\partial t}\frac{\partial\delta w}{\partial t} + I_0 B^2\frac{\partial^3 w}{\partial x^2\partial t}\frac{\partial^3\delta w}{\partial x^2\partial t}\end{array}\right]dx \\ &= \int_0^L \left[-I_0\frac{\partial^2 u}{\partial t^2}\delta u - \left(-I_2\frac{\partial^4 w}{\partial x^2\partial t^2} + I_0\frac{\partial^2 w}{\partial t^2} + 2I_0 B\frac{\partial^4 w}{\partial x^2\partial t^2} + B^2 I_0\frac{\partial^6 w}{\partial x^4\partial t^2}\right)\delta w\right]dx\end{aligned} \tag{19}$$

in which $I_0 = \int_0^{2\pi}\int_0^r \rho(rdrd\theta) = \rho A$ and $I_2 = \int_0^{2\pi}\int_0^r \rho(r\sin\theta)^2(rdrd\theta) = \rho I$, are called mass moments of inertia. As far as the linear analysis is adopted, the I_1 would be ignored.

The virtual work done (δW) by external loads such as longitudinal magnetic field, nonlinear thermal environment, and the hygroscopic environment is obtained as

$$\delta W = \int_0^L \left[\eta A H_x^2\left(\frac{\partial^2 w}{\partial x^2}\right) - \left(EA\beta_x\Delta H\right)\left(\frac{\partial^2 w}{\partial x^2}\right) - \left(EA\alpha_x\Delta T - A\hat{h}\alpha_x^2\Delta T^2\right)\left(\frac{\partial^2 w}{\partial x^2}\right)\right]\delta w dx \tag{20}$$

Replacing Eqs. (18-20) into the extended Hamilton's principle $\delta\prod = \int_0^t \delta(W - U + T)dt$ and setting $\delta\prod$ to zero, the equations of motion can be presented as

$$\frac{\partial N_{xx}}{\partial x} = I_0\frac{\partial^2 u}{\partial t^2} \tag{21.a}$$

$$\left[\begin{array}{l}\frac{\partial^2 M_{xx}}{\partial x^2} + B\frac{\partial^3 Q_{xz}}{\partial x^3} + \eta A H_x^2\left(\frac{\partial^2 w}{\partial x^2}\right) - \left(EA\alpha_x\Delta T - A\hat{h}\alpha_x^2\Delta T^2\right)\left(\frac{\partial^2 w}{\partial x^2}\right) \\ -\left(EA\beta_x\Delta H\right)\left(\frac{\partial^2 w}{\partial x^2}\right) + I_2\frac{\partial^4 w}{\partial x^2\partial t^2} - I_0\left(\frac{\partial^2 w}{\partial t^2} + 2B\frac{\partial^4 w}{\partial x^2\partial t^2} + B^2\frac{\partial^6 w}{\partial x^4\partial t^2}\right)\end{array}\right] = 0 \tag{21.b}$$

From the Hookean stress-strain elasticity relation we have

$$M_{xx} = -EI\frac{\partial^2 w}{\partial x^2}$$
$$Q_{xz} = AGB\frac{\partial^3 w}{\partial x^3} \tag{22}$$

From the nonlocal strain gradient theory, i.e., from Eq. (3), we have

$$\left(1-(e_0 a)^2\frac{\partial^2}{\partial x^2}\right)\sigma_{ij} = C_{ijkl}\left(1-l^2\frac{\partial^2}{\partial x^2}\right)\varepsilon_{kl} \tag{23}$$

in which $\sigma_{ij}, \varepsilon_{kl}$ and C_{ijkl} are stress tensor, strain tensor, and elastic modulus constant, respectively.

From Eq. (22) and Eq. (23), the nonlocal stress resultants may be obtained as

$$\left(1-(e_0 a)^2\frac{\partial^2}{\partial x^2}\right)M_{xx} = -EI\left(\frac{\partial^2 w}{\partial x^2}-l^2\frac{\partial^4 w}{\partial x^4}\right) \tag{24.a}$$

$$\left(1-(e_0 a)^2\frac{\partial^2}{\partial x^2}\right)Q_{xz} = AGB\left(\frac{\partial^3 w}{\partial x^3}-l^2\frac{\partial^5 w}{\partial x^5}\right) \tag{24.b}$$

Implementing Eq. (24) in Eq. (21), the governing equation of motion is obtained as

$$\left(1-(e_0 a)^2\frac{\partial^2}{\partial x^2}\right)\begin{bmatrix}\left(EA\alpha_x\Delta T - A\hat{h}\alpha_x^2\Delta T^2\right)\left(\frac{\partial^2 w}{\partial x^2}\right)-I_2\frac{\partial^4 w}{\partial x^2\partial t^2}\\ -\eta AH_x^2\left(\frac{\partial^2 w}{\partial x^2}\right)+\left(EA\beta_x\Delta H\right)\left(\frac{\partial^2 w}{\partial x^2}\right)\\ +I_0\left(\frac{\partial^2 w}{\partial t^2}+2B\frac{\partial^4 w}{\partial x^2\partial t^2}+B^2\frac{\partial^6 w}{\partial x^4\partial t^2}\right)\end{bmatrix} = \left\langle\begin{matrix}AGB^2\left(\frac{\partial^6 w}{\partial x^6}-l^2\frac{\partial^8 w}{\partial x^8}\right)\\ -EI\left(\frac{\partial^4 w}{\partial x^4}-l^2\frac{\partial^6 w}{\partial x^6}\right)\end{matrix}\right\rangle \tag{25}$$

By setting gradient parameter $l=0$, the above equation i.e. Eq.(25) will be reduced into the governing equation of motion for NET. Similarly, by letting nonlocal parameter $e_0 a = 0$, we will obtain the governing equation of motion for SGT. When both the nonlocal and gradient parameters $e_0 a = l = 0$, the Eq. (25) will be modified into the governing equation of CET.

3. Analytical method

In this investigation, Navier's approach has been employed on the governing equation, i.e., Eq. (25) to compute the frequency parameters of SWCNTs for the Hinged-Hinged (HH) boundary condition. As per Navier's approach, the transverse displacement $w(x,t)$ can be presented as [Malikan *et al.*, 2019]

$$w(x,t) = \sum_{n=1}^{\infty} W_n \sin\left(\frac{n\pi}{L}x\right)e^{i\omega_n t}, \tag{26}$$

where W_n, and ω_n are amplitude of the transverse displacement and frequency of the SWCNTs.

Substituting Eq. (26) into Eq. (25), the frequency parameters $\left(\omega_n^2\right)$ may be obtained as

$$\omega_n^2 = \frac{\left[1+(e_0a)^2\left(\frac{n\pi}{L}\right)^2\right]\left[\begin{array}{l}\left(A\hat{h}\alpha_x^2\Delta T^2 - EA\alpha_x\Delta T\right)\left(\frac{n\pi}{L}\right)^2 \\ +\eta AH_x^2\left(\frac{n\pi}{L}\right)^2 - EA\beta_x\Delta H\left(\frac{n\pi}{L}\right)^2\end{array}\right] + \left[1+l^2\left(\frac{n\pi}{L}\right)^2\right]\left[(EI)\left(\frac{n\pi}{L}\right)^4 + AGB^2\left(\frac{n\pi}{L}\right)^6\right]}{\left[1+(e_0a)^2\left(\frac{n\pi}{L}\right)^2\right]\left[I_2\left(\frac{n\pi}{L}\right)^2 + I_0 - 2BI_0\left(\frac{n\pi}{L}\right)^2 + B^2I_0\left(\frac{n\pi}{L}\right)^4\right]} \tag{27}$$

Again simplifying Eq. (27), we have

$$\omega_n^2 = \frac{\left[\left(\frac{n\pi}{L}\right)^2 + (e_0a)^2\left(\frac{n\pi}{L}\right)^4\right]\left[\eta AH_x^2 + A\hat{h}\alpha_x^2\Delta T^2 - EA\alpha_x\Delta T - EA\beta_x\Delta H\right] + \left[\left(\frac{n\pi}{L}\right)^4 + l^2\left(\frac{n\pi}{L}\right)^6\right]\left[(EI) + AGB^2\left(\frac{n\pi}{L}\right)^2\right]}{\left[1+(e_0a)^2\left(\frac{n\pi}{L}\right)^2\right]\left[I_2\left(\frac{n\pi}{L}\right)^2 + I_0 - 2BI_0\left(\frac{n\pi}{L}\right)^2 + B^2I_0\left(\frac{n\pi}{L}\right)^4\right]} \tag{28}$$

4. Results and discussion

In this investigation, zigzag type SWCNT is taken into consideration having chirality indices $(21, 0)$. The corresponding diameter is $d = 1.64nm$, which is calculated by using the expression $d = \frac{a}{\pi}\sqrt{3(n^2+m^2+mn)}$ as given in Zhen and Fang [2010], where $a = 0.142nm$, is the C-C bond length. The non-dimensional frequency parameters $\left(\Omega_n = \omega_n L^2\sqrt{\frac{I_0}{EI}}\right)$ have been computed for the Hinged-Hinged (HH) boundary condition using the Navier's approach. We have acquired Young's modulus $E = 1TPa$, thickness of the SWCNT $h = 0.34nm$, mass density $\rho = 1370Kg/m^3$, and Poisson's ratio $\nu = 0.19$ from Zhen and Fang, [2010] as well as the magnetic permeability $\eta = 4\pi\times10^{-7}\,H/m$ and the magnetic field intensity $H_x = 4\times10^8\,A/m$ from Zhen *et al.* [2019]. Similarly, coefficient of thermal expansion $\alpha_x = 2.1\times10^{-6}\,K^{-1}$ and coefficient of hygroscopic expansion $\beta_x = 0.0026(\text{wt.\% of } H_2O)^{-1}$ are taken from Karami *et al.* [2019].

4.1. Validation

As there is no existing model similar to the proposed problem, the validation of the present model is conducted by comparing the non-dimensional frequency parameters with the existing model in special cases. In this regard, hygroscopic environment, thermal environment, magnetic field, and gradient parameter, and B are neglected, and frequency parameters of HH boundary conditions are compared with Jena and Chakraverty [2018], which is demonstrated in Table 1. Further, to verify the refined beam model, numerical outcomes of the present work are also compared with the results of molecular dynamics study [Mehralian *et al.*, 2017], in special cases, which is depicted in Table 2. For the calculation of numerical results, $E = 1.06TPa$, $\upsilon = 0.19$, and $d = 0.68nm$ are considered with nonlocal parameters taken as $e_0a = 3.3$ to $3.5nm$. It may be noted that the first-order of shear

deformation model in a shell domain for the carbon nanotube has been taken in [Mehralian *et al.*, 2017] for Hinged-Hinged boundary condition. From Tables 1-2, one may observe an excellent agreement between the present and existing results for both computational and molecular dynamics study.

Table 1. Validation of present model with Jena and Chakraverty [2018] in special cases.

$(e_0a)^2$ in nm^2	$\sqrt{\Omega_1}$			$\sqrt{\Omega_2}$			$\sqrt{\Omega_3}$		
	Present	[A]	[B]	Present	[A]	[B]	Present	[A]	[B]
0	3.1416	3.1416	0	6.2832	6.2832	0	9.4248	9.4248	0
1	3.0685	3.0685	0	5.7817	5.7817	0	8.0399	8.0400	0.0012
2	3.0032	3.0032	0	5.4324	5.4324	0	7.3012	7.3012	0
3	2.9444	2.9444	0	5.1683	5.1683	0	6.8117	6.8118	0.0014
4	2.8908	2.8908	0	4.9580	4.9581	0.002	6.4520	6.4520	0

[A]: Jena and Chakraverty [2018], [B]: % difference in results

Table 2. Comparison of natural frequencies (THz) for a nanotube

L/d	[C]	Eringen's nonlocal elasticity theory			
		[D]	Present, [Malikan *et al.*, 2018a]	% difference with [C]	% difference with [D]
4.86	1.138	0.758	0.759	33.3040	0.1319
8.47	0.466	0.333	0.354	24.0343	6.3063
13.89	0.190	0.165	0.163	14.2105	1.2121
17.47	0.122	0.121	0.124	1.6393	2.4793

[C]: [Mehralian *et al.*, 2017] (MD), [D]: [Mehralian *et al.*, 2017] (ENET)

4.2. Effect of nonlocal parameter

In this subsection, the effect of nonlocal parameter (e_0a) on the non-dimensional frequency parameters has been studied. As the NSGT is the generalization of CET, NET, and SGT, graphical results for CET, NET, and SGT are also presented. From computational purpose, rise in Temp. $(\Delta T)=50\,K$, change in moisture concentration $(\Delta H)=1\,(\text{wt.\% of } H_2O)$, and length of SWCNT $(L)=10\,nm$ are taken. The effects of nonlocal parameter (e_0a) have been investigated on frequency parameters corresponding to CET, NET, SGT, and NSGT, which are illustrated in Figs. 4-6. From these results, it is observed that the non-dimensional frequency parameters are decreasing with increase in nonlocal parameter for NET, and NSGT whereas the frequency parameters for CET and SGT remain constant as these two theories are size-independent with respect to nonlocal parameter. Among these four theories, SGT possesses the highest value of non-dimensional frequency parameters, while NET is having the lowest value of non-dimensional frequency parameters. For the lower value of nonlocal parameters, the difference between NSGT and SGT is less, but this difference becomes much more prominent for the higher value of nonlocal parameter. This trend is exactly the same for CET and NET. As a matter of fact, about decreasing trend of results due to enhancing in values of nonlocal parameter, one can say that in the differential formulation of Eringen $\left[\left(1-(e_0a)^2\frac{\partial^2}{\partial x^2}\right)\sigma_{ij}=C_{ijkl}\varepsilon_{kl}\right]$ when the stress is decreased, the strain is increased. This will result in a softening effect. Consequently, the increase of nonlocal parameter leads to decreasing of the natural frequencies.

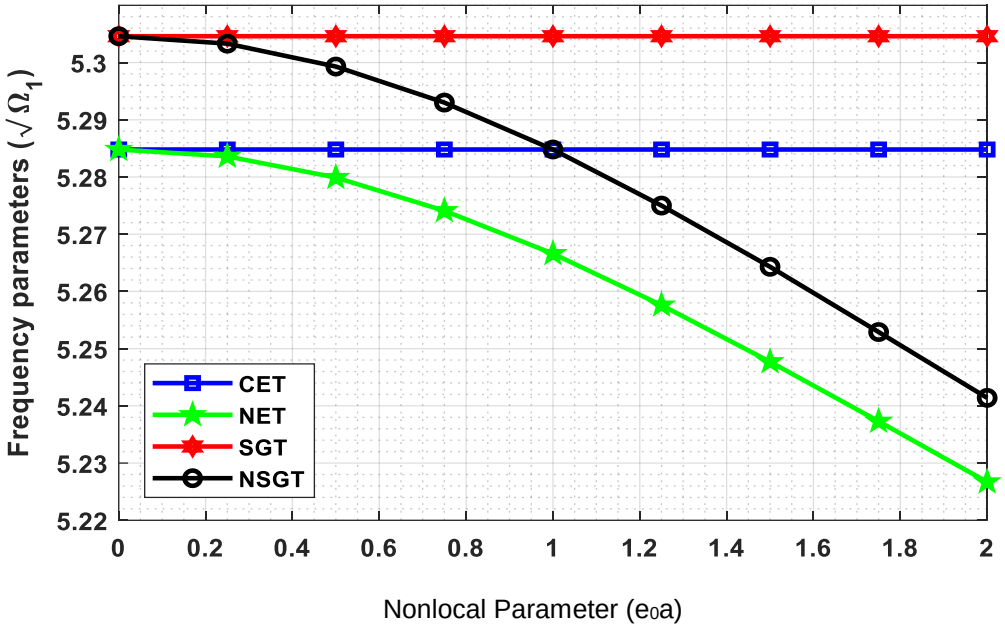

Fig. 4. First mode frequency parameter Vs. nonlocal parameter

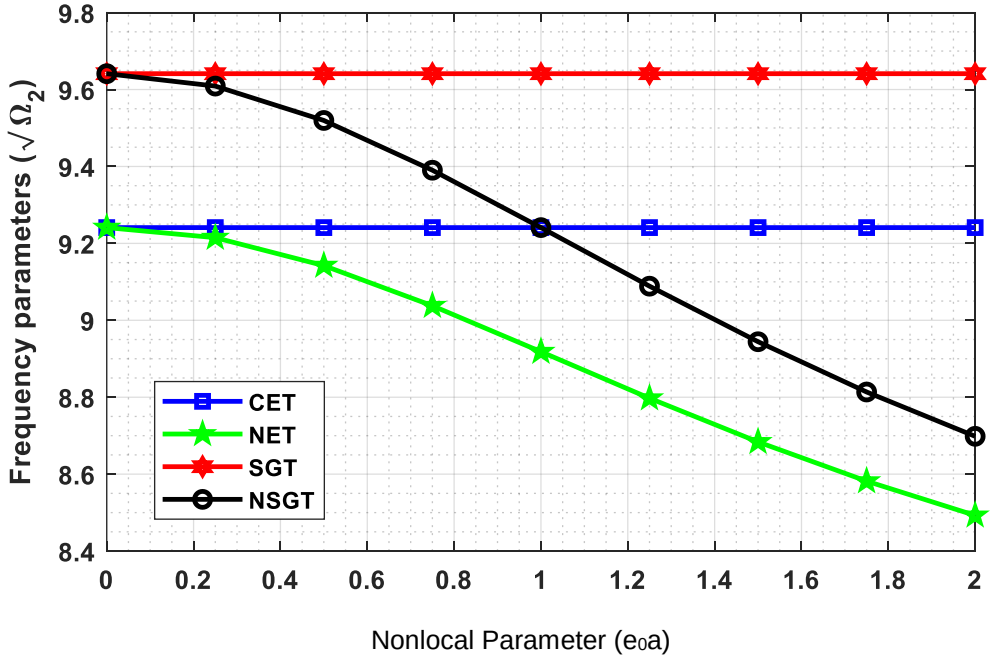

Fig. 5. Second mode frequency parameter Vs. nonlocal parameter

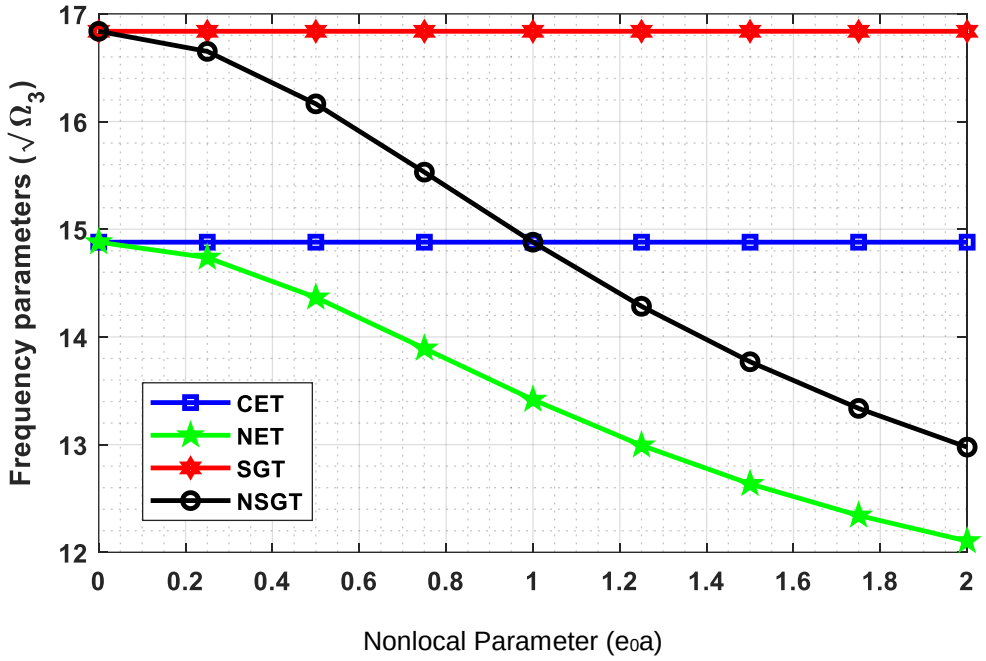

Fig. 6. Third mode frequency parameter Vs. nonlocal parameter

4.3. Effect of gradient parameter

Through this subsection, the influence of gradient parameter (l) is analyzed on non-dimensional frequency parameters corresponding to CET, NET, SGT, and NSGT, which are depicted in Figs. 7-9. For the computation of the graphical results, change in Temp. $(\Delta T)=50\,K$, change in moisture concentration $(\Delta H)=1\,(\text{wt.}\,\%\,\text{of}\,H_2O)$, and length of SWCNT $(L)=10\,nm$ are taken into consideration. The gradient parameter is varied from $0\,nm$ to $2\,nm$ with an increment of $0.25\,nm$ to capture the microstructure effect. From these graphical results, it is opined that the non-dimensional frequency parameters for NSGT and SGT are increasing when the gradient parameter (l) gets larger, whereas non-dimensional frequency parameters of CET and NET remain unchanged as both the theories don't incorporate microstructure effect. The non-dimensional frequency parameters computed by the SGT are higher than those of NSGT as SGT captures more microstructure effects than NSGT. Also, when the gradient parameter (l) becomes one, the non-dimensional frequency parameters for CET and NSGT match with each other. As a matter of fact, about increasing trend of results due to enhancing in values of gradient parameter, one can write that in the differential formulation of Mindlin $\left[\sigma_{ij}=C_{ijkl}\left(1-l^2\frac{\partial^2}{\partial x^2}\right)\varepsilon_{kl}\right]$ when the stress is increased, the strain is decreased. This will result in a hardening effect. Consequently, the increase of gradient parameter leads to increasing of the natural frequencies.

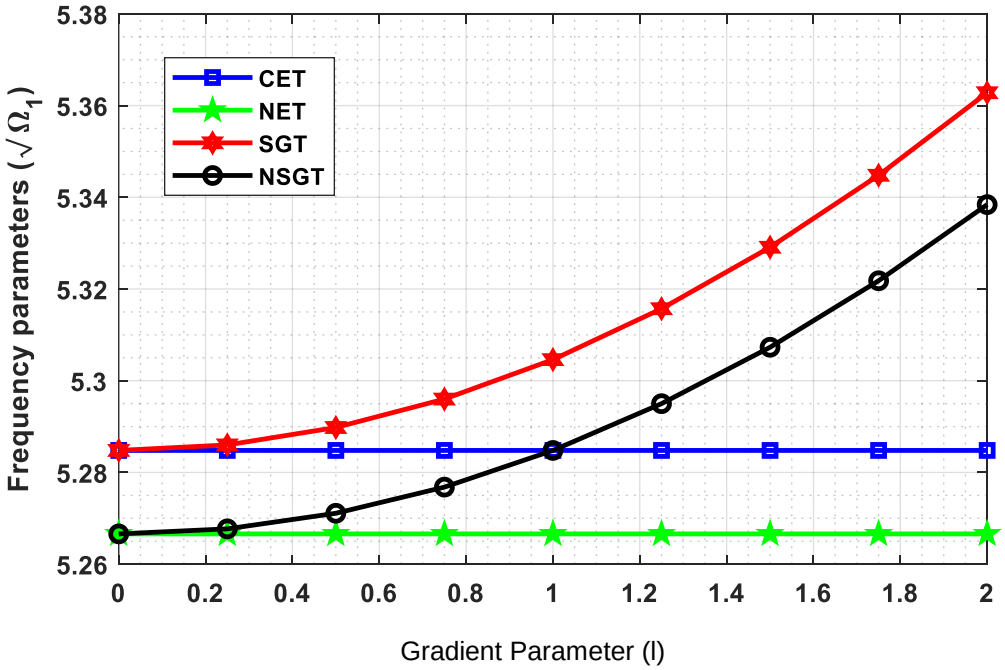

Fig. 7. First mode frequency parameter Vs. gradient parameter

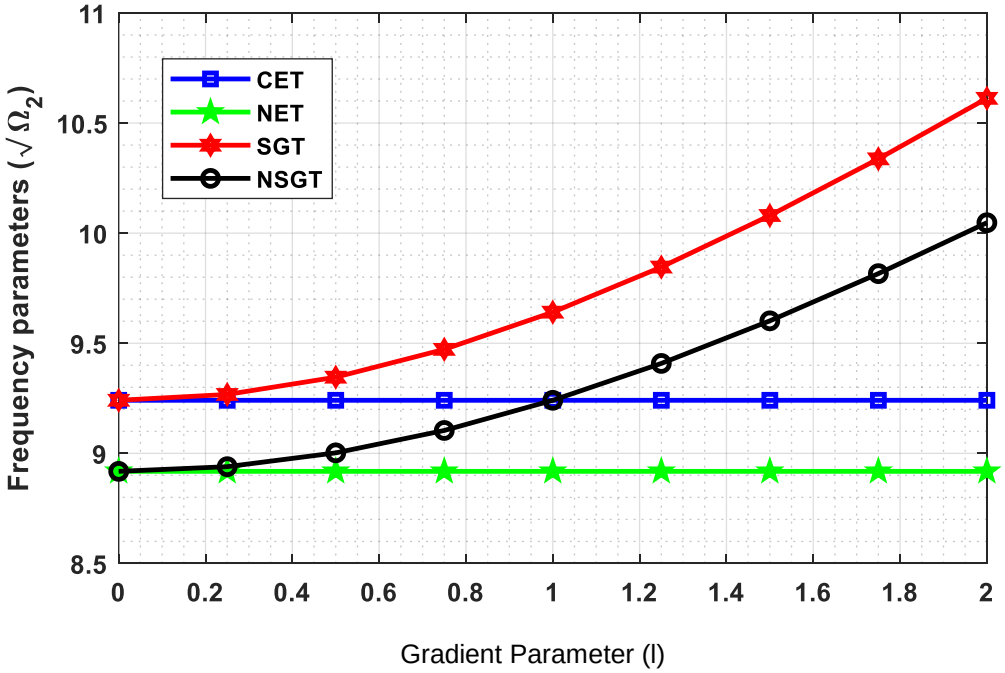

Fig. 8. Second mode frequency parameter Vs. gradient parameter

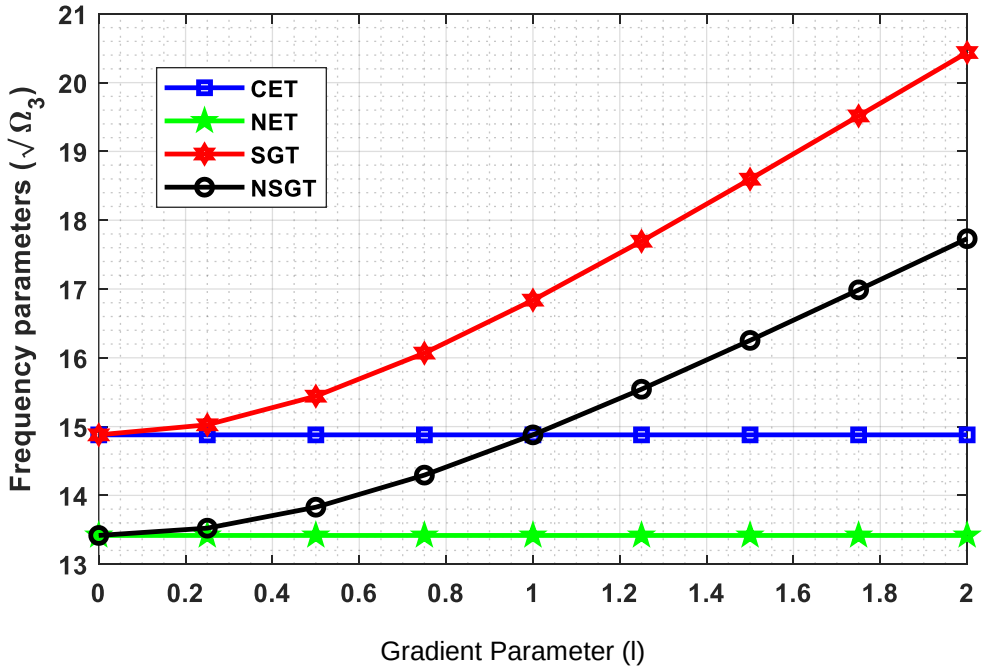

Fig. 9. Third mode frequency parameter Vs. gradient parameter

4.4. Effect of thermal environment

In this subsection, the impact of the rise in Temp. (ΔT) on non-dimensional frequency parameters have been discussed by considering several elasticity theories, which are specified as CET, NET, SGT, NSGT with $(l > e_0 a)$ and NSGT with $(e_0 a > l)$ as well as both the linear and nonlinear distribution of temperatures. The rise in Temp. (ΔT) is varied from $0K$ to $400K$, with an increase of $50K$ and the change in moisture concentration $(\Delta H) = 1$ (wt. % of H_2O), and length of SWCNT $(L) = 10nm$ are considered in this study. In this regard, graphical results are plotted by varying change in Temp. (ΔT) with respect to $\chi_{\Delta T}$, which represent the ratio of non-dimensional frequency parameters with change in Temp. and non-dimensional frequency parameters without change in Temp. i.e. $\chi_{\Delta T} = \dfrac{\sqrt{\Omega_n}\ \text{with}\ \Delta T \neq 0}{\sqrt{\Omega_n}\ \text{with}\ \Delta T = 0}$. From Figs. 10-12, it is very evident that non-dimensional frequency parameters are decreasing with the increase in ΔT for both the linear and nonlinear temperature environment, and this decrease is more prominent in the case of higher modes. Also, the nonlinear thermal distribution environment possesses higher non-dimensional frequencies corresponding to the linear thermal environment. Physically, temperature makes the atoms and molecules far from each other and they will scatter across the whole material. This means that the material will be softer in a thermal environment and the stiffness becomes lower. That is why when the temperature gets higher, the natural frequency values get lower.

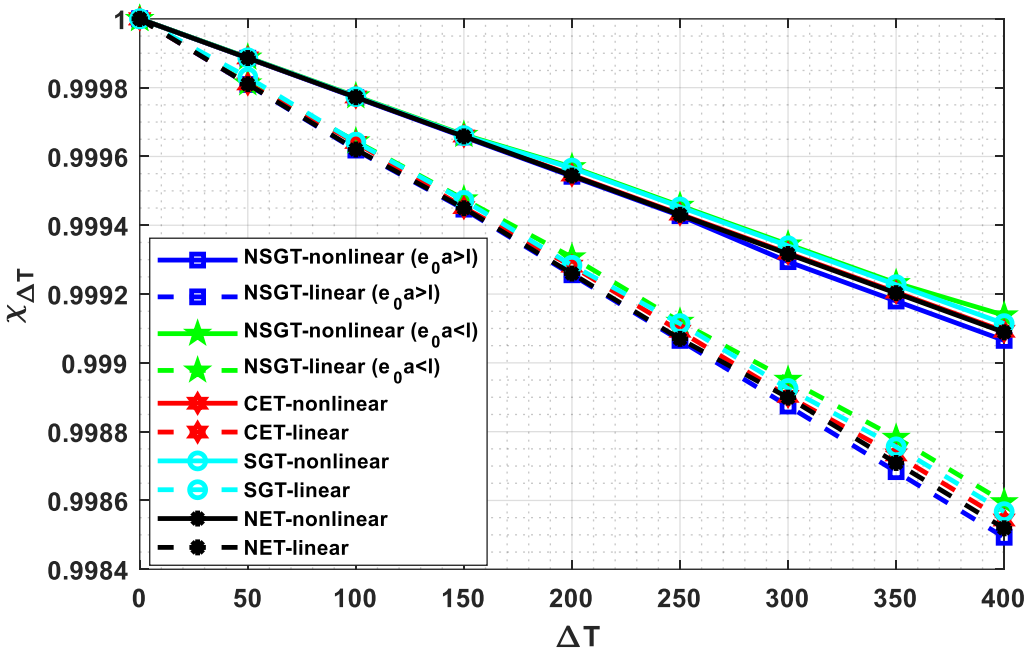

Fig. 10. $\chi_{\Delta T}$ Vs. temperature variations for first mode

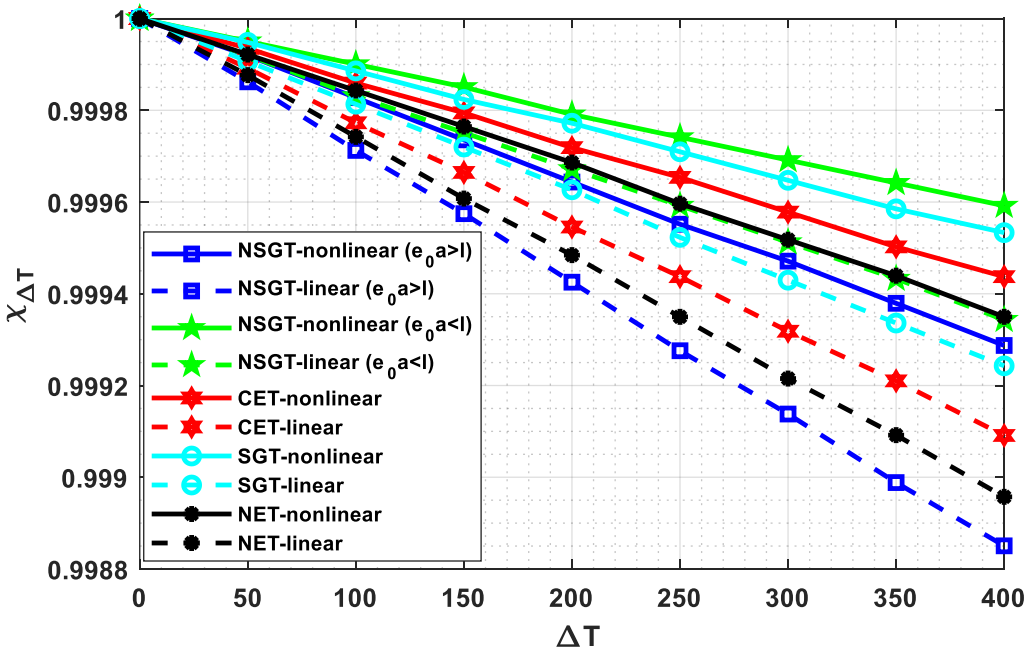

Fig. 11. $\chi_{\Delta T}$ Vs. temperature variations for second mode

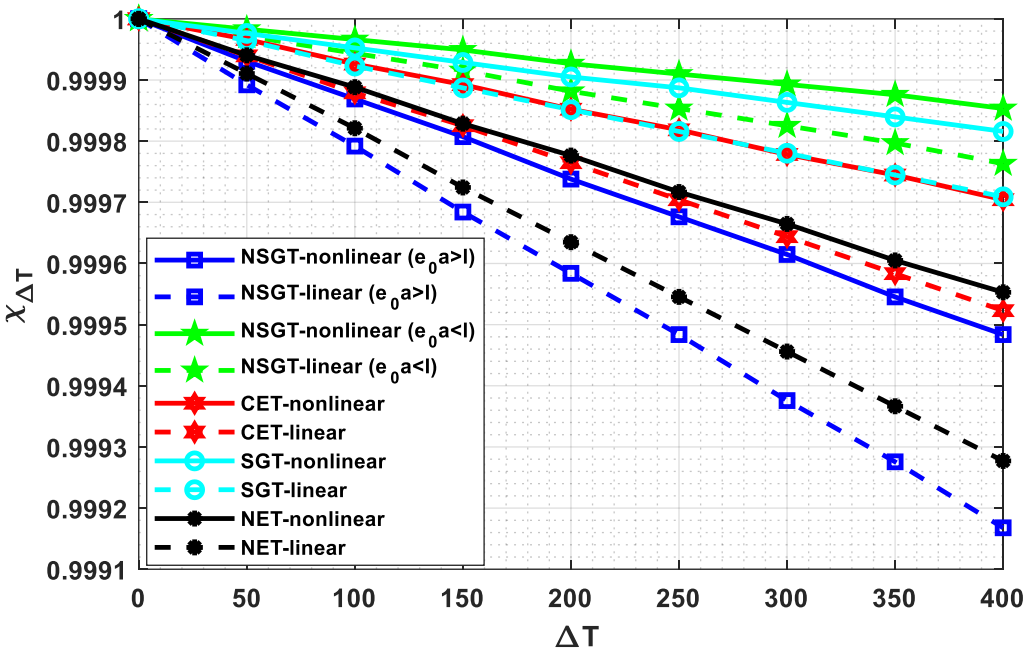

Fig. 12. $\chi_{\Delta T}$ Vs. temperature variations for third mode

4.5. Effect of hygroscopic environment

This subsection is aimed to discuss the effect of hygroscopic environment or change in moisture concentration (ΔH)on non-dimensional frequency parameters corresponding to different elasticity theories like CET, NET, SGT, NSGT with $(l > e_0 a)$ and NSGT with $(e_0 a > l)$. Concerning this, graphical results are plotted by varying ΔH from $0\,(\text{wt.\%of } H_2O)$ to $4\,(\text{wt.\%of } H_2O)$ with an increment of $0.5\,(\text{wt.\%of } H_2O)$ while taking $\Delta T = 100\,K$ and $L = 10\,nm$. The graphical results which are illustrated in Figs. 13-15, represent the variation $\chi_{\Delta H}$ $\left(\chi_{\Delta H} = \dfrac{\sqrt{\Omega_n}\ \text{with}\ \Delta H \neq 0}{\sqrt{\Omega_n}\ \text{with}\ \Delta H = 0}\right)$ with respect to ΔH. From these results, one may note that rise in moisture concentration (ΔH) reduces non-dimensional frequency parameters for all the elasticity theories, and these effects are more remarkable in higher modes. Physically, it can be interpreted that the moisture concentration into the material can be like some vacancies between molecules and atoms which are filled with water molecules. Naturally, this would lead to weakening the resistance of the structure and subsequently the natural frequencies. It is germane to say that the moisture has a remarkable effect on the small scale response of the nanostructure. This is due to the gap increasing between the results of the CET and several small scale approaches by augmenting the humidity. It can be stated the nanostructure can act as a hygral-dependent material as well.

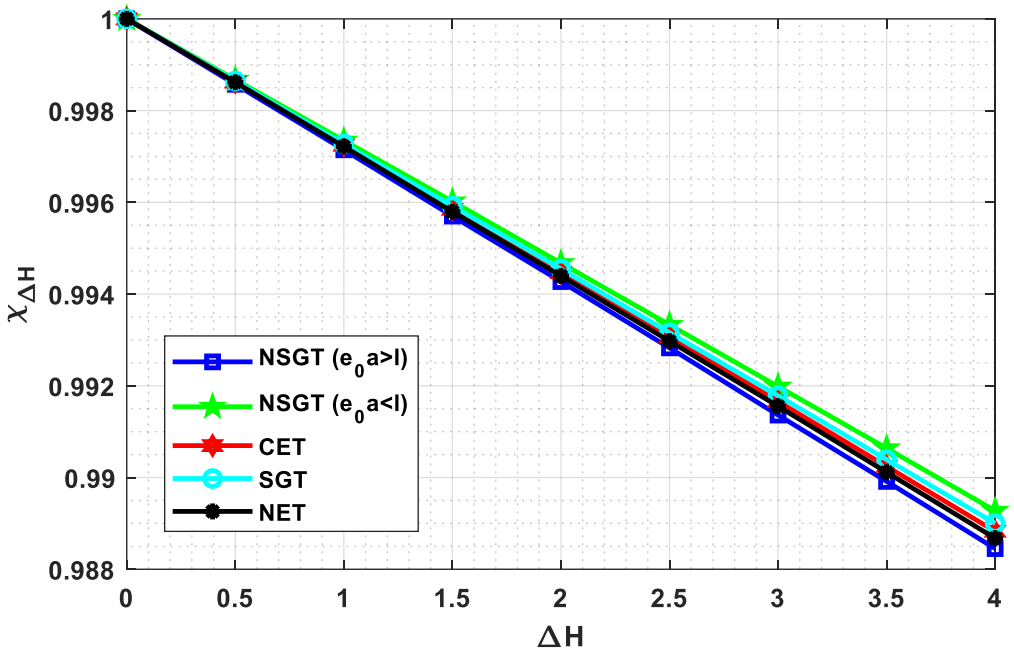

Fig. 13. $\chi_{\Delta H}$ Vs. hygral variations for first mode

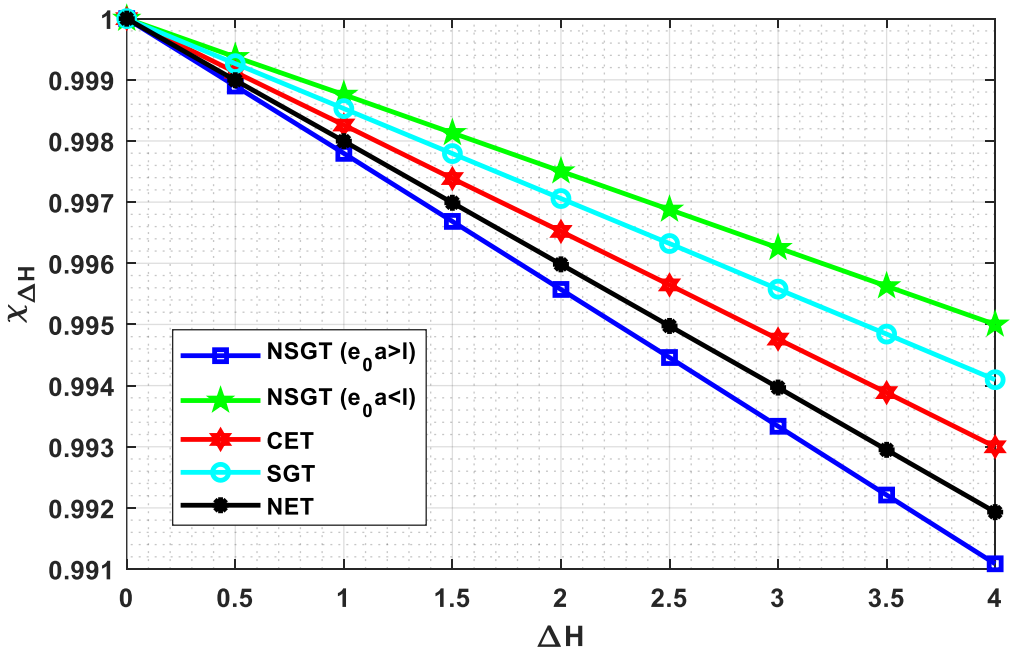

Fig. 14. $\chi_{\Delta H}$ Vs. hygral variations for second mode

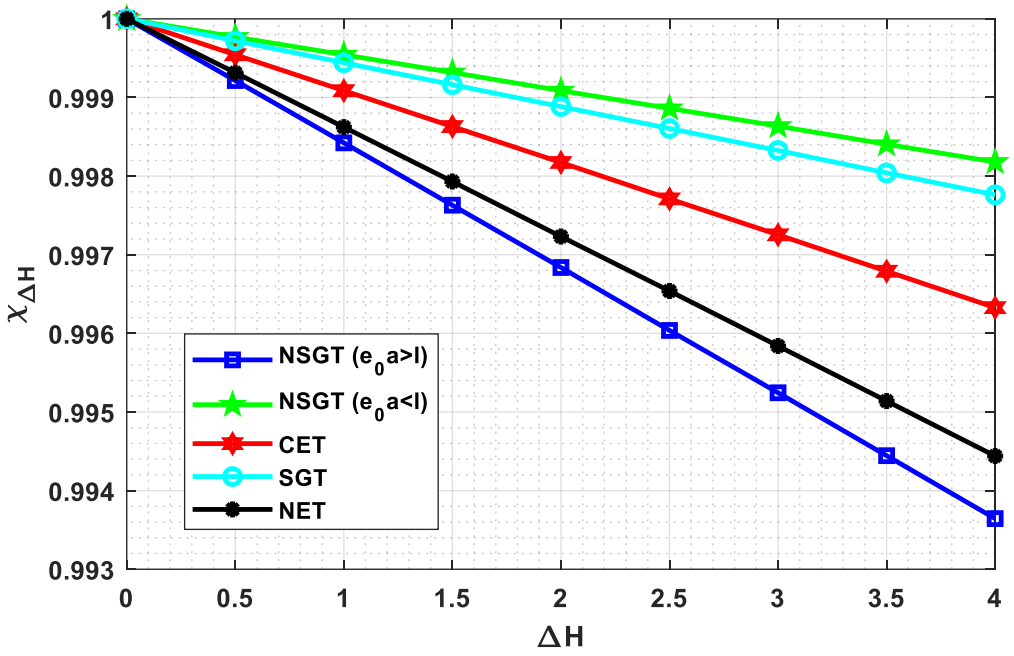

Fig. 15. $\chi_{\Delta H}$ Vs. hygral bariations for third mode

4.6. Effect of magnetic field intensity

The influence of magnetic field intensity (H_x) on non-dimensional frequency parameters has been studied through this subsection. Various elasticity theories such as CET, NET, SGT, NSGT with $(l > e_0 a)$ and NSGT with $(e_0 a > l)$, have been considered in this investigation. The influence of magnetic field intensity (H_x) is varied from $0\times10^8\ A/m$ to $10\times10^8\ A/m$ with an increment of $2\times10^8\ A/m$ whereas $\Delta T = 100K$, $\Delta H = 1\,(\text{wt.\% of } H_2O)$, and length of SWCNT $L = 10nm$. The graphical results are plotted in Figs. 16-18 by varying χ_{H_X} with H_X and It may be noted that χ_{H_X} is the ratio of non-dimensional frequency parameter with magnetic field effect and non-dimensional frequency parameter without magnetic field. These results reveal that the non-dimensional frequency parameters are increasing when H_X gets larger and this trend is the same for all the elasticity theories but more prominent in higher modes. It is also observed that by considering high magnetic field, the gap between outputs of CET and small scale approaches would be enhanced leads to this finding that in a strong magnetic field the small scale effect would be a vital phenomenon. Physically, when a material with magneto-mechanical coupling feature is placed into a magnetic field, the molecules and atoms get closer to one another in whole the material. In short, the material will be shortened as a result of contraction which leads to a material with further resistance. That is why by an increase in the magnetis potential the material will be stronger resulting in higher natural frequencies.

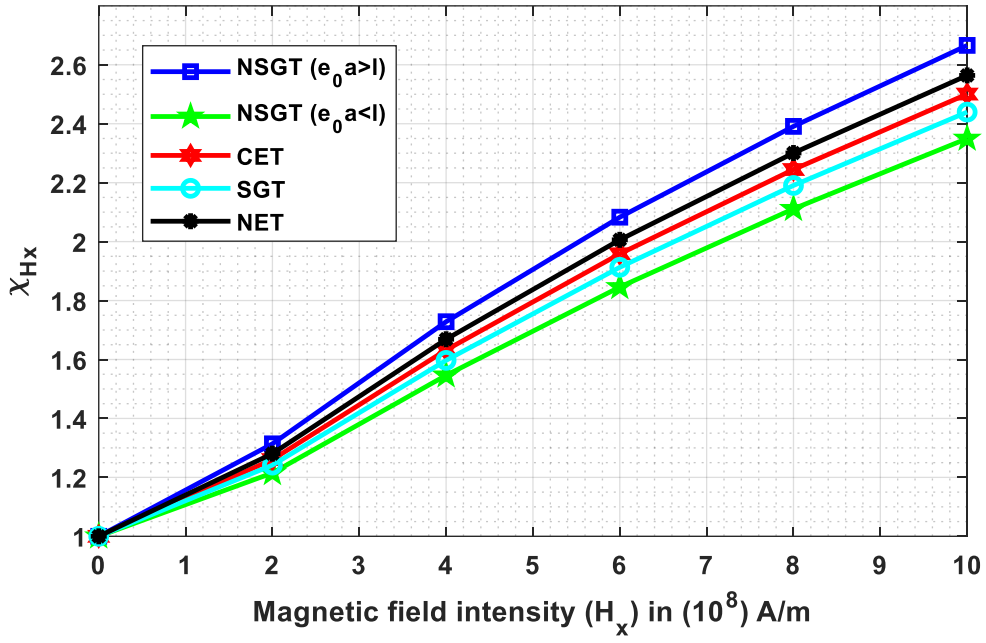

Fig. 16. χ_{H_X} Vs. magnetic field intensity for first mode

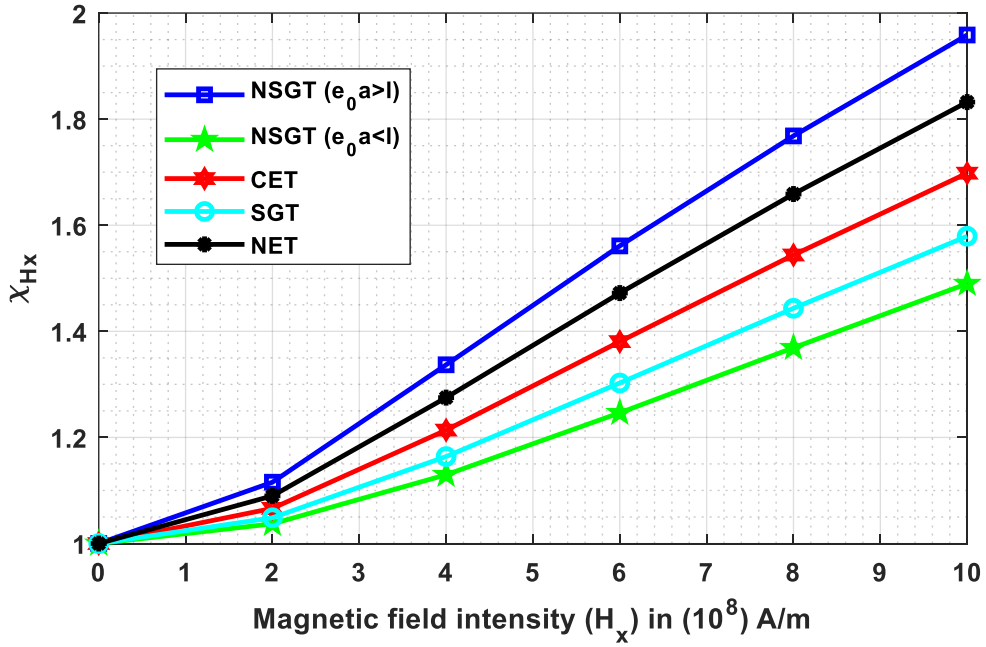

Fig. 17. χ_{H_X} Vs. magnetic field intensity for second mode

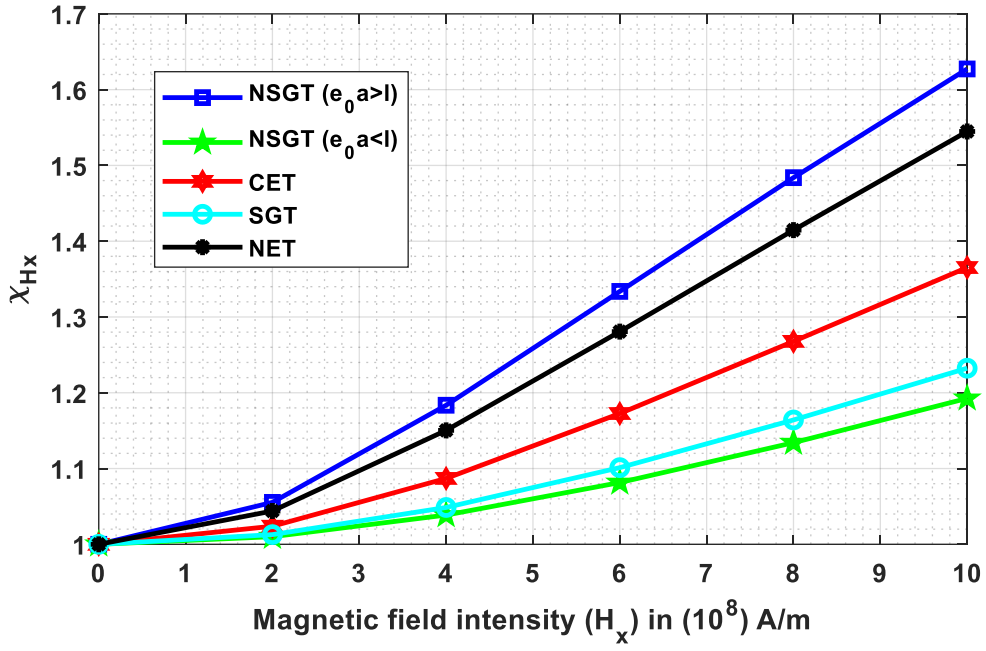

Fig. 18. χ_{H_x} Vs. magnetic field intensity for third mode

5. Concluding remarks

In the present investigation, Navier's approach has been implemented to analyze the vibration characteristics of SWCNT, which is placed in a longitudinal magnetic field and is also exposed to both the nonlinear thermal environment and linear hygroscopic environment. A new refined beam theory has been incorporated to develop the model, whereas and the size effect of SWCNT is captured by NSGT. The governing equation of motion of the proposed model has been developed by utilizing the extended Hamilton's principle, and the non- dimensional frequency parameters have been computed for Hinged-Hinged (HH) boundary condition. The proposed model is validated with the existing model in special cases, displaying an excellent agreement. Further, a parametric study has been conducted to investigate the impact of various parameters. Following are the main comments;

- The non-dimensional frequency parameters are decreasing with an increase in nonlocal parameter for NET, and NSGT whereas the frequency parameters for CET and SGT remain constant.
- The non-dimensional frequency parameters for NSGT and SGT are increasing when the gradient parameter gets larger, whereas non-dimensional frequency parameters of CET and NET remain unchanged as both the theories don't incorporate microstructure effect.
- NSGT with $(l > e_0a)$ is having the highest value of non-dimensional frequency while NSGT with $(e_0a > l)$ possesses the least value. The frequency parameters of NET and NSGT with $(e_0a > l)$ are matching with each other in higher modes when the slenderness ratio gets larger. The same trend is also observed for SGT and NSGT with $(l > e_0a)$.
- The non-dimensional frequency parameters are decreasing with the increase in change in Temp. (ΔT) for both the linear and nonlinear temperature environments and this decrease is more prominent in the case of higher modes. Also, the nonlinear thermal distribution environment possesses higher non-dimensional frequencies corresponding to the linear thermal environment.
- The rise in moisture concentration (ΔH) reduces non-dimensional frequency parameters for all the elasticity theories, and these effects are more remarkable in higher modes.
- The non-dimensional frequency parameters are increasing when the magnetic field intensity (H_x)gets larger, and this trend is the same for all the elasticity theories but more prominent in higher modes.

- Nanoscale size materials other than size-dependent can be considered as temperature-dependent structures. This means, external temperature fundamentally affects the small scale behavior. And the higher temperature the environment, the larger the nanoscale impact.
- It is observed that the nanobeam can respond as a hygral-dependent structure.
- The importance of small scale effect can be completely confirmed whilst a strong magnetic field is taken into consideration.

Acknowledgment

The first two authors would like to acknowledge Defence Research & Development Organization (DRDO), New Delhi, India (Sanction Code: DG/TM/ERIPR/GIA/17-18/0129/020) for the funding to carry out the present research work.

References

Akgöz, B. and Civalek, O. [2012] "Free vibration analysis for single-layered graphene sheets in an elastic matrix via modified couple stress theory," *Materials and Design* **42**, 164-171.

Akgöz, B. and Civalek, O. [2014] "Longitudinal vibration analysis for microbars based on strain gradient elasticity theory," *Journal of Vibration and Control* **20**, 606-616.

Alibeigi, B., Beni, Y. T. and Mehralian, F. [2018] "On the thermal buckling of magneto-electro-elastic piezoelectric nanobeams," *The European Physical Journal Plus* **133**(3), 133.

Ansari, R. and Gholami, R. [2014] "Size-Dependent Nonlinear Vibrations of First-Order Shear Deformable Magneto-Electro-Thermo Elastic Nanoplates Based on the Nonlocal Elasticity Theory," *International Journal of Applied Mechanics* **06**, 1450011.

Ansari, R., Ajori, S. and Arash, B. [2012] "Vibrations of single- and double-walled carbon nanotubes with layerwise boundary conditions: A molecular dynamics study," *Current Applied Physics* **12**, 707-711.

Apuzzo, A., Barretta, R., Faghidian, S. A., Luciano, R. and Marotti de Sciarra, F. [2018] "Free vibrations of elastic beams by modified nonlocal strain gradient theory," *International Journal of Engineering Science* **133**, 99-108.

Arani, A. G., Dashti, P., Amir, S. and Yousefi, M. [2015] "Flexural vibration of coupled double-walled Carbon nanotubes conveying fluid under thermo-magnetic fields based on strain gradient theory," *Journal of Theoretical and Applied Mechanics* **53**, 947-957.

Arefi, M. and Soltan Arani, A. H. [2018] "Higher order shear deformation bending results of a magnetoelectrothermoelastic functionally graded nanobeam in thermal, mechanical, electrical, and magnetic environments," *Mechanics Based Design of Structures and Machines* **46**(6), 669-692.

Arunachalam, S., Gupta, A. A., Izquierdo, R. and Nabki, F. [2018] "Suspended carbon nanotubes for humidity sensing," *Sensors* **18**(5), 1655.

Arunachalam, S., Izquierdo, R., Nabki, F. [2019] "Low-Hysteresis and Fast Response Time Humidity Sensors Using Suspended Functionalized Carbon Nanotubes," *Sensors* **19**, 680.

Aydogdu, M. and Filiz, S. [2011] "Modeling carbon nanotube-based mass sensors using axial vibration and nonlocal elasticity," *Physica E: Low-Dimensional Systems and Nanostructures* **43**, 1229-1234.

Barati, M. R., Faleh, N. M. and Zenkour, A. M. [2019] "Dynamic response of nanobeams subjected to moving nanoparticles and hygro-thermal environments based on nonlocal strain gradient theory," *Mechanics of Advanced Materials and Structures* **26**(19), 1661-1669.

Barretta R. [2012] "On the relative position of twist and shear centres in the orthotropic and fiberwise homogeneous Saint-Venant beam theory," *International Journal of Solids and Structures* **49**, 3038-3046.

Barretta R. [2013] "Analogies between Kirchhoff plates and Saint-Venant beams under torsion," *Acta Mechanica* **224**, 2955-2964.

Barretta R. [2014] "Analogies between Kirchhoff plates and Saint-Venant beams under flexure," *Acta Mechanica* **225**, 2075-2083.

Barretta, R. and Marotti de Sciarra, F. [2018] "Constitutive boundary conditions for nonlocal strain gradient elastic nano-beams," *International Journal of Engineering Science* **130**, 187-198.

Barretta, R., Faghidian, S. A., Marotti de Sciarra, F. and Vaccaro, M.S. [2020] "Nonlocal strain gradient torsion of elastic beams: variational formulation and constitutive boundary conditions," *Archive of Applied Mechanics* **90**, 691-706.

Cao, C. L., Hu, C. G., Fang, L., Wang, S. X., Tian, Y. S. and Pan, C. Y. [2011] "Humidity Sensor Based on Multi-Walled Carbon Nanotube Thin Films," *Journal of Nanomaterials* doi.org/10.1155/2011/707303.

Chang, T. P. [2017] "Nonlinear vibration of single-walled carbon nanotubes with nonlinear damping and random material properties under magnetic field," *Composites Part B: Engineering* **114**, 69-79.

Demir, C. and Civalek, O. [2017] "On the analysis of microbeams," *International Journal of Engineering Science*," **121**, 14-33.

Dini, A., Zandi-Baghche-Maryam, A. and Shariati, M. [2019] "Effects of van der Waals forces on hygro-thermal vibration and stability of fluid-conveying curved double-walled carbon nanotubes subjected to external magnetic field," *Physica E: Low-Dimensional Systems and Nanostructures* **106**, 156-169.

Ebrahimi, F. and Barati, M. R. [2017a] "Magnetic field effects on nonlocal wave dispersion characteristics of size-dependent nanobeams," *Applied Physics A* **123**(1), 81.

Ebrahimi, F. and Barati, M. R. [2017b] "Small-scale effects on hygro-thermo-mechanical vibration of temperature-dependent nonhomogeneous nanoscale beams," *Mechanics of Advanced Materials and Structures* **24**(11), 924-936.

Ebrahimi, F. and Dabbagh, A. [2019] "Vibration analysis of multi-scale hybrid nanocomposite plates based on a Halpin-Tsai homogenization model," *Composites Part B: Engineering* **173**, 106955.

Ebrahimi-Nejad, S., Shaghaghi, G. R., Miraskari, F. and Kheybari, M. [2019] "Size-dependent vibration in two-directional functionally graded porous nanobeams under hygro-thermo-mechanical loading," *The European Physical Journal Plus* **134**(9), 465.

Eltaher, M. A., Agwa, M. A. and Kabeel, A. [2018] "Vibration Analysis of Material Size-Dependent CNTs Using Energy Equivalent Model," *Journal of Applied and Computational Mechanics* **4**, 75-86.

Eltaher, M. A., Almalki, T. A., Ahmed, K. I. E. and Almitani, K. H. [2019a] "Characterization and behaviors of single walled carbon nanotube by equivalent-continuum mechanics approach," *Advances in Nano Research* **7**, 39-49.

Eltaher, M. A., Omer, F. A., Abdella, W. S. and Gad, E. H. [2019b] "Bending and vibrational behaviors of piezoelectric nonlocal nanobeam including surface elasticity," *Waves in Random and Complex Media* **29**, 264-280.

Eringen, A. C. [1972] "Linear theory of non-local elasticity and dispersion of plane waves, *International Journal of Engineering Sciences*," **10**, 425-435.

Habibi, B., Beni, Y. T. and Mehralian, F. [2019] "Free vibration of magneto-electro-elastic nanobeams based on modified couple stress theory in thermal environment," *Mechanics of Advanced Materials and Structures* **26**(7), 601-613.

Han, J. W., Kim, B., Li, J. and Meyyappan, M. [2012] "Carbon nanotube based humidity sensor on cellulose paper," *The Journal of Physical Chemistry C* **116**(41), 22094-22097.

Huang, J.R., Li, M.Q., Huang, Z., Liu, J.H. [2009] "A novel conductive humidity sensor based on field ionization from carbon nanotubes," *Sensors and Actuators A: Physical*, **133**(2), 467-471.

Islam, ZM., Jia, P. and Lim, CW. [2014] "Torsional wave propagation and vibration of circular nanostructures based on nonlocal elasticity theory," *International Journal of Applied Mechanics* **06**, 1450011.

Jalaei, M. H., Arani, A. G. and Nguyen-Xuan, H. [2019] "Investigation of thermal and magnetic field effects on the dynamic instability of FG Timoshenko nanobeam employing nonlocal strain gradient theory," *International Journal of Mechanical Sciences* **161**, 105043.

Je¸kot, T. [1996] "Nonlinear problems of thermal postbuckling of a beam," *Journal of thermal stresses* **19**(4), 359-367.

Jena, S. K. and Chakraverty, S. [2018] "Free vibration analysis of Euler–Bernoulli nanobeam using differential transform method," *International Journal of Computational Materials Science and Engineering* **7**(03), 1850020.

Jena, S. K. and Chakraverty, S. [2019] "Dynamic behavior of an electromagnetic nanobeam using the Haar wavelet method and the higher-order Haar wavelet method," *The European Physical Journal Plus* **134**(10), 538.

Jena, S. K., Chakraverty, S. and Malikan, M. [2020a] "Implementation of non-probabilistic methods for stability analysis of nonlocal beam with structural uncertainties," *Engineering with Computers* 2020. https://doi.org/10.1007/s00366-020-00987-z

Jena, S. K., Chakraverty, S. and Malikan, M. [2020b] "Vibration and buckling characteristics of nonlocal beam placed in a magnetic field embedded in Winkler–Pasternak elastic foundation using a new refined beam theory: an analytical," *The European Physical Journal Plus* **135**, 164.

Jena, S. K., Chakraverty, S., Malikan, M. and Tornabene, F. [2019a] "Stability analysis of single-walled carbon nanotubes embedded in winkler foundation placed in a thermal environment considering the surface effect using a new refined beam theory," *Mechanics Based Design of Structures and Machines* 1-15.

Jena, S. K., Chakraverty, S. and Tornabene, F. [2019b] "Buckling Behavior of Nanobeams Placed in Electromagnetic Field Using Shifted Chebyshev Polynomials-Based Rayleigh-Ritz Method," *Nanomaterials* **9**(9), 1326.

Jena, S. K., Chakraverty, S. and Jena, R. M. [2019c] "Propagation of uncertainty in free vibration of Euler–Bernoulli nanobeam," *Journal of the Brazilian Society of Mechanical Sciences and Engineering* **41**(10), 436.

Jena, S. K., Chakraverty, S. and Malikan, M. [2019d] "Implementation of Haar wavelet, higher order Haar wavelet, and differential quadrature methods on buckling response of strain gradient nonlocal beam embedded in an elastic medium," *Engineering with Computers*, 1-14.

Jouneghani, F. Z., Dimitri, R. and Tornabene, F. [2018] "Structural response of porous FG nanobeams under hygro-thermo-mechanical loadings," *Composites Part B: Engineering* **152**, 71-78.

Jung, D., Han, M. and Lee, G. S. [2014] "Humidity-sensing characteristics of multi-walled carbon nanotube sheet" *Materials Letters* **122**, 281-284.

Karami, B., Shahsavari, D., Janghorban, M. and Li, L. [2019] "Wave dispersion of nanobeams incorporating stretching effect," *Waves in Random and Complex Media* 1-21.

Khaniki, H. B. and Hosseini-Hashemi, S. [2017] "Buckling analysis of tapered nanobeams using nonlocal strain gradient theory and a generalized differential quadrature method," *Materials Research Express* **4**(6), 065003.

Kiani, K. [2012] "Transverse wave propagation in elastically confined single-walled carbon nanotubes subjected to longitudinal magnetic fields using nonlocal elasticity models," *Physica E: Low-dimensional Systems and Nanostructures* **45**, 86-96.

Kiani, K. [2018] "Nonlocal free dynamic analysis of periodic arrays of single-walled carbon nanotubes in the presence of longitudinal thermal and magnetic fields," *Computers & Mathematics with Applications* **75**(11), 3849-3872.

Kraus, J. D. [1984] *Electromagnetics*. USA, McGraw Hill.

Lim, C. W., Zhang, G. and Reddy, J. N. [2015] "A higher-order nonlocal elasticity and strain gradient theory and its applications in wave propagation," *Journal of the Mechanics and Physics of Solids* **78**, 298-313.

Li, L., Hu, Y. and Ling, L. [2016] "Wave propagation in viscoelastic single-walled carbon nanotubes with surface effect under magnetic field based on nonlocal strain gradient theory," *Physica E: Low-dimensional Systems and Nanostructures* **75**, 118-124.

Lu, L., Guo, X. and Zhao, J. [2017] "Size-dependent vibration analysis of nanobeams based on the nonlocal strain gradient theory," *International Journal of Engineering Science* **116**, 12-24.

Luciano, R., Caporale, A., Darban, H. and Bartolomeo, C. [2020] "Variational approaches for bending and buckling of non-local stress-driven Timoshenko nano-beams for smart materials," *Mechanics Research Communications* **103**, 103470.

Ma, Y., Ma, S., Wang, T. and Fang, W. [1995] "Air-flow sensor and humidity sensor application to neonatal infant respiration monitoring," *Sensors and Actuators A: Physical* **49**(1-2), 47-50.

Ma, L. H., Ke, L. L., Wang, Y. Z. and Wang, Y. S. [2017] "Wave propagation in magneto-electro-elastic nanobeams via two nonlocal beam models," *Physica E: Low-dimensional Systems and Nanostructures* **86**, 253-261.

Maachou, M., Zidour, M., Baghdadi, H., Ziane, N. and Tounsi, A. [2011] "A nonlocal Levinson beam model for free vibration analysis of zigzag single-walled carbon nanotubes including thermal effects," *Solid State Communications* **151**(20), 1467-1471.

Malikan, M. [2017] "Electro-mechanical shear buckling of piezoelectric nanoplate using modified couple stress theory based on simplified first order shear deformation theory," *Applied Mathematical Modelling* **48**, 196-207.

Malikan, M. [2020] "On the plastic buckling of curved carbon nanotubes," *Theoretical and Applied Mechanics Letters* **10**, 46-56.

Malikan, M., Krasheninnikov, M. and Eremeyev, V. A. [2020] "Torsional stability capacity of a nano-composite shell based on a nonlocal strain gradient shell model under a three-dimensional magnetic field," *International Journal of Engineering Science* **148**, 103210.

Malikan, M., Dimitri, R. and Tornabene, F. [2019] "Transient response of oscillated carbon nanotubes with an internal and external damping," *Composites Part B: Engineering* **158**, 198-205.

Mehralian, F., Beni, Y. T. and Zeverdejani, M. K. [2017] "Nonlocal strain gradient theory calibration using molecular dynamics simulation based on small scale vibration of nanotubes," *Physica B: Condensed Matter* **514**, 61-69.

Mindlin, R. D. [1965] "Second gradient of train and surface-tension in linear elasticity, *International Journal of Solids and Strucutres*," **1**, 417-438.

Mindlin, R. D. and Eshel, N. N. [1968] "On first strain-gradient theories in linear elasticity," *International Journal of Solids and Strucutres* **4**, 109-124.

Mohamed, N., Mohamed, S. A. and Eltaher, M. A. [2020] "Buckling and post-buckling behaviors of higher order carbon nanotubes using energy-equivalent model," *Engineering with Computers*. https://doi.org/10.1007/s00366-020-00976-2

Mohammadi, M., Safarabadi, M., Rastgoo, A. and Farajpour, A [2016] "Hygro-mechanical vibration analysis of a rotating viscoelastic nanobeam embedded in a visco-Pasternak elastic medium and in a nonlinear thermal environment," *Acta Mechanica* **227**(8), 2207-2232.

Moraes, M. C., Galeazzo, E., Peres, H. E., Ramirez-Fernandez, F. J. and Dantas, M. O. [2014] "Development of fast response humidity sensors based on carbon nanotubes," In *Proc. IEEE 5th Int. Conf. Sensor Device Technol. Appl.*, 7-10.

Mouffoki, A., Bedia, E. A., Houari, M. S. A., Tounsi, A. and Mahmoud, S. R. [2017] "Vibration analysis of nonlocal advanced nanobeams in hygro-thermal environment using a new two-unknown trigonometric shear deformation beam theory," *Smart Structures and Systems* **20**(3), 369-383.

Narendar, S., Gupta, S. S. and Gopalakrishnan, S. [2012] "Wave propagation in single-walled carbon nanotube under longitudinal magnetic field using nonlocal Euler–Bernoulli beam theory,". *Applied Mathematical Modelling* **36**(9), 4529-4538.

Numano□lu, H. M., Akgöz, B. and Civalek, O. [2018] "On dynamic analysis of nanorods," *International Journal of Engineering Science* **130**, 33-50.

Ponnusamy, P. and Amuthalakshmi, A. [2015] "Influence of thermal and magnetic field on vibration of double walled carbon nanotubes using nonlocal Timoshenko beam theory," *Procedia Materials Science* **10**, 243-253.

Pradhan, S. C. and Mandal, U. [2013] "Finite element analysis of CNTs based on nonlocal elasticity and Timoshenko beam theory including thermal effect," *Physica E: Low-Dimensional Systems and Nanostructures* **53**, 223-232.

Quelennec, A., Duchesne, É., Frémont, H. and Drouin, D. [2019] "Source Separation Using Sensor's Frequency Response: Theory and Practice on Carbon Nanotubes Sensors," *Sensors* **19**(15), 3389.

Romano G., Barretta A. and Barretta R. [2012] "On torsion and shear of Saint-Venant beams," *European Journal of Mechanics A/Solids* **35**, 47-60.

Takahashi, S. [2018] "Measurement of third-order elastic constants and stress dependent coefficients for steels," *Mechanics of Advanced Materials and Modern Processes* **4**(1), 2.

Thai, C.-H., Zenkour, A. M., Wahab, M. A. and Nguyen-Xuan, H. [2016] "A simple four-unknown shear and normal deformations theory for functionally graded isotropic and sandwich plates based on isogeometric analysis," *Composite Structures* **139**, 77-95.

Yazdani, R., Mohammadimehr, M. and Navi, B. R. [2019] "Free vibration of Cooper-Naghdi micro saturated porous sandwich cylindrical shells with reinforced CNT face sheets under magneto-hydro-thermo-mechanical loadings," *Structural Engineering and Mechanics* **70**, 351-365.

Zeighampour, H. and Tadi Beni, Y. [2014] "Size-dependent vibration of fluid-conveying double-walled carbon nanotubes using couple stress shell theory," *Physica E: Low-dimensional Systems and Nanostructures* **61**, 28-39.

Zhao, Z. G., Liu, X. W., Chen, W. P. and Li, T. [2011] "Carbon nanotubes humidity sensor based on high testing frequencies," *Sensors and Actuators A: Physical* **168**(1), 10-13.

Zhen, Y. and Fang, B. [2010] "Thermal–mechanical and nonlocal elastic vibration of single-walled carbon nanotubes conveying fluid" *Computational Materials Science* **49**(2), 276-282.

Zhen, Y. X., Wen, S. L. and Tang, Y. [2019] "Free vibration analysis of viscoelastic nanotubes under longitudinal magnetic field based on nonlocal strain gradient Timoshenko beam model," *Physica E: Low-dimensional Systems and Nanostructures* **105**, 116-124.

Zidour, M., Benrahou, K. H., Semmah, A., Naceri, M., Belhadj, H. A., Bakhti, K. and Tounsi, A. [2012] "The thermal effect on vibration of zigzag single walled carbon nanotubes using nonlocal Timoshenko beam theory," *Computational materials science* **51**(1), 252-260.